Investigation of effects of sand particles on aerodynamic performance of NACA 0012 airfoil

NACA 0012 kanat profilinin aerodinamik performansı üzerinde toz partiküllerinin etkilerinin incelenmesi

Fuat Kaya[1,*] 📷

[1] *Niğde Ömer Halisdemir University, Department of Mechanical Engineering, 51240, Niğde, Türkiye*

Abstract

The purpose of this paper is to study the effects of turbulence kinetic energy structures formed during flow and particles of different diameters and different flow velocities in the air in different regional areas on aerodynamic performance characteristics in NACA 0012. Single and two phase fluid flows were worked out by using Ansys Fluent Computational Fluid Dynamics (CFD) code. Computational results obtained from Ansys Fluent CFD code for pure air and the air containing sand particles were compared with numerical values gained in the literature for validation. Results obtained from the numerical tests demonstrate good agreement with the value in the literature. These results indicate the turbulence kinetic energy value occurred in the tail region of the airfoil increases with the increase in the angle of attack and shifts towards the upper region of the airfoil at high attack angle. Moreover, the upper region of the airfoil at high attack angle becomes larger at low Reynolds numbers due to viscous effects. The drag and lift coefficients obtained in the numerical tests of the airfoils and in the experimental tests in the wind tunnel will differ from the values in the application area. Because, in the operation of airfoils in different regional environments, there are always particles of various concentrations and diameters in the air. In this case, the drag coefficient increases and the lift coefficient decreases.

Keywords: Airfoil, Turbulence kinetic energy, CFD, Drag coefficient, Lift coefficient

Öz

Bu çalışmanın amacı, NACA 0012'de akış sırasında oluşan türbülans kinetik enerji yapılarının ve havadaki farklı çaplardaki ve farklı akış hızlarındaki parçacıkların farklı bölgesel alanlarda aerodinamik performans özelliklerine etkilerini incelemektir. Tek ve iki fazlı akışkan akışları çalışılmıştır. Ansys Fluent Hesaplamalı Akışkanlar Dinamiği (CFD) kodunu kullanarak. Saf hava ve kum parçacıkları içeren hava için elde edilen hesaplama sonuçları, doğrulama için literatürde elde edilen sayısal değerlerle karşılaştırılmıştır. Sayısal testlerden elde edilen sonuçlar, literatürdeki değer ile iyi bir uyum göstermektedir. Bu sonuçlar kanat profilinin kuyruk bölgesinde meydana gelen türbülans kinetik enerji değerinin hücum açısının artmasıyla arttığını ve yüksek hücum açısında kanat profilinin üst bölgesine doğru kaydığını göstermektedir. Ayrıca, yüksek hücum açısında kanat profilinin üst bölgesi, düşük Reynolds sayılarında viskoz etkilerden dolayı genişlemektedir. Kanat profillerinin sayısal testlerinde ve rüzgar tünelinde deneysel testlerde elde edilen sürükleme ve kaldırma katsayıları, uygulama alanındaki değerlerden farklılık gösterecektir. Çünkü kanat profillerinin farklı bölgesel ortamlarda çalışmasında, havada her zaman çeşitli konsantrasyonlarda ve çaplarda parçacıklar bulunmaktadır. Bu durumda sürükleme katsayısı artmakta ve kaldırma katsayısı azalmaktadır.

Anahtar kelimeler: Kanat profili, Türbülans kinetik enerjisi, HAD, Direnç katsayısı, Kaldırma katsayısı

1 Introduction

Aerodynamics is a branch of science that has emerged to examine the movements of objects exposed to air flow and to determine their optimum characteristics. In other words, Aerodynamics is defined as the study of the resulting effects of relative motion between air molecules and surfaces [1]. In particular, the design and optimization of aircraft is very important in order to meet the needs of developing technology and increasing population. In this context, the carrying capacity of aircraft used for various purposes emerges depending on the determination of the lift and drag coefficients of the airfoils.

Optimum characteristics of airfoils in aircraft are obtained by having a high lift coefficient and a low drag coefficient. Many studies have been done on this subject. These studies were carried out numerically mainly due to the rapid development in computational fluid dynamics.

Douvi et al. [2] examined the NACA 0012 airfoil for different angles of attack and turbulence models when the Reynolds number is $3x10^6$. They stated that computational fluid dynamics turbulence models are not sufficient to obtain results at high angles of attack.

Adel [3] numerically investigated pressure distributions, lift and drag forces at different angles of attack using three different geometries, NACA 0012, NACA 2412 and SG

6043. He used the k-ω SST turbulence model in his numerical solutions. He stated that the SG 6043 airfoil is more suitable for wind turbine applications.

Bodavula et al. [4] worked at low Reynolds numbers using the NACA 0012 airfoil profile to evaluate micro-scale aircraft for military and civil unmanned aerial vehicles. In their study, they analyzed the different triangular protrusion values of the NACA 0012 airfoil. They showed that for low triangular protrusion values, the lift characteristics were significantly improved, especially at high angles of attack.

Iliev et al. [5] studied the difference experimentally and numerically on NACA 0015 in terms of speed and angle of attack. They showed that optimum performance was achieved at 8° angle of attack at different entry speeds.

The performance characteristics of micro scale and high altitude unmanned aerial vehicles and wind turbines are highly affected by laminar separation at low Reynolds numbers [6-8].

Rogowski et al. [9] tested how close the numerical tests performed with different turbulence models on the NACA 0018 airfoil were to the experimental results. They stated that the results obtained with the Transition SST turbulence model are much more agreement with the experimental results.

Umapathi and Soni [10] numerically studied NACA 2313 and NACA 7322 airfoils. They made their study by comparing the lift, drag and pressure coefficients for 6° and 10° angles of attack. In the results obtained, they evaluated the NACA 2313 airfoil as superior to the NACA 7322 airfoil.

Singh [11] worked on NACA 6, TsAGI 'B' series and Hortex brother's airfoils. Performance analyzes were made by considering the lift and drag coefficients of the airfoil. He noted that Hortex brother's airfoils provide more lift and less drag compared to other airfoils.

Rubel et al. [12] compared NACA 0015 and NACA 4415 airfoil profiles numerically and experimentally at $0° \leq \alpha \leq 18°$ angles of attack. They stated that the non-symmetrical NACA 4415 airfoil is aerodynamically more favorable than NACA 0015 airfoil.

Pranto and Inam [13] considered the NACA 4312 airfoil at different angles of attack and turbulence models, with a constant Reynolds number. It was observed that the k-Ɛ and k-ω turbulence models gave almost similar results, both lift and drag coefficients increased at higher angles of attack, but the lift coefficient began to decrease at $\alpha = 13°$, known as the stopping condition.

Dhivyadharshini et al. [14] investigated the aerodynamic efficiency situation by considering the effects of roughness on the NACA 2412 airfoil. They considered the triangular surface roughness at the trailing edge to be the most suitable surface modification.

Shabur et al. [15] performed aerodynamic analysis of symmetrical type NACA 0018 and NACA 0012 airfoils at different Reynolds numbers and angles of attack. They stated that the optimum angle of attack was 10° and the C_L/C_D ratio increased by the Reynolds number. They also showed that at the same Reynolds numbers, the NACA 0012 airfoil provided more lift than the NACA 0018 airfoil. Thus, they stated that NACA 0012 airfoil would be more suitable for air

vehicles and NACA 0018 airfoil would be more suitable for wind energy applications.

As can be seen from the above studies in the literature, there are many studies on airfoils under various geometric and operating parameters, and it is desired to determine the optimum aerodynamic parameters. These studies are for single phase air environment. However, when the working environments of the airfoils are taken into account, not only single phase air, but also different environments such as air-particle, air-rain, air-snow are encountered. This situation is effective on the aerodynamic performance characteristics of the airfoil and there are very few studies on this subject in the literature. Some of these studies are given below.

Fatahian et al. [16] performed aerodynamic performance analysis on the NACA 0012 airfoil under dry and rainy weather conditions. In their study, they stated that there are significant decreases in the aerodynamic performance of the airfoil, especially at low angles of attack in rainy weather. In addition, they stated that the sound pressure level increased with the increase of the angle of attack, especially in the frequency regions higher than 2500 Hz under rainy conditions.

Heavy rains have negative effects on vehicle aerodynamics and maneuverability [17-19].

When the small number of literature on the operation of airfoils in different environments is examined, we come across environments with a different air-sand concentration.

Douvi et al. [20] performed numerical tests for 1.76×10^6 Reynolds number, different angles of attack and single-phase airflow and dual-phase air-sand flow on the NACA 0012 airfoil. They used Realizable k–ε as turbulence model and Discrete Phase Model (DPM) for particle injection. They showed that the sand concentration in the air affects the wing aerodynamics, in such cases the lift force decreases and the drag force increases.

In this study, it is aimed to determine the optimum aerodynamic performance characteristics of the NACA 0012 airfoil in different operating environments (air, air+particle). In order to determine these characteristics, numerical tests were carried out at different particle diameters, attack angles and Reynolds numbers.

2 Material and method

2.1 Numerical approach

In accordance with the studies of Douvi et al. [20], studies were carried out for a symmetrical NACA 0012 airfoil as thick as 12% of the cord length.

In the calculation area, a geometric structure has been applied so that the height is equal to 25 beam lengths. In order to better determine the aerodynamic effects on the airfoil, solutions have been obtained by adding 1000 times denser mesh to the areas close to the airfoil than the other areas. In addition, the independence tests from the mesh number were performed and the final solutions were obtained at 175000 nodes.

The mesh independence tests were performed at 5° angles of attack and Re=1.76×10^6 (Table 1).

Mesh structures used in numerical tests are given in Figures 1 and 2. Numerical tests were performed using

Ansys Fluent commercial software to solve the conservation equations under continuous, incompressible and turbulent flow conditions. Realizable k-ε turbulence model was used as turbulence model.

Table 1. Mesh independence tests

Node Numbers	C_D
68700	0.02098
114780	0.01345
175000	**0.01336**
228790	0.01340
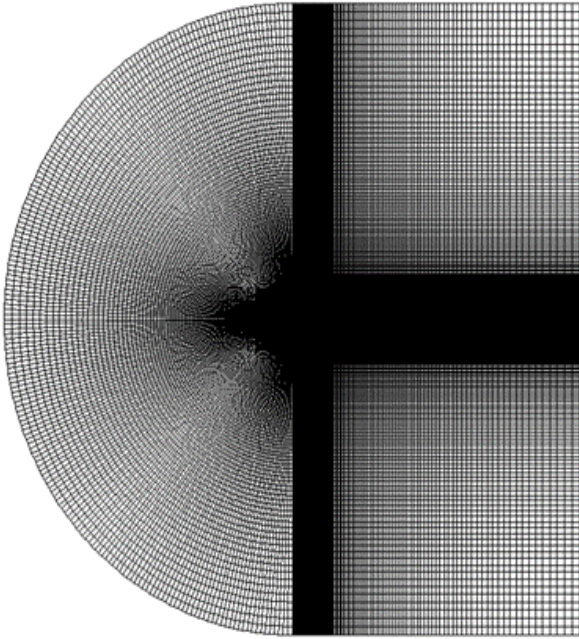
Figure 1. Structured C-Type mesh structure
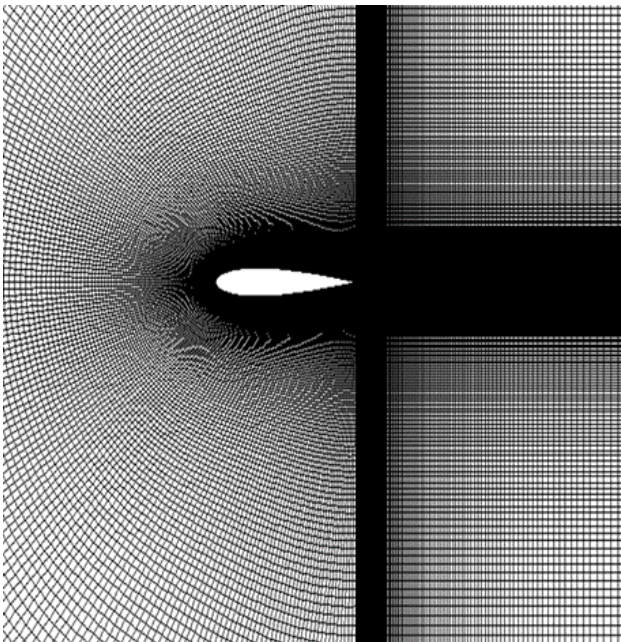
Figure 2. Close-up view of the dense mesh structure around the airfoil

2.2 Particle approach

Air-sand phase flow on the NACA 0012 airfoil is modeled using the Lagrangian Discrete Phase Model (DPM). As a solution approach, the change in momentum of a sand particle across each control volume is calculated by the following equation [20]:

$$F = \sum \left(\frac{18\mu C_D Re}{\rho_p d_p^2 24} (u_p - u) + F_{other} \right) \dot{m}_p \Delta t \qquad (1)$$

In accordance with the studies of Douvi et al. [20], where µ is the viscosity of the fluid, C_D the drag coefficient, Re the relative Reynolds number, ρ_p the density of the particle, d_p the diameter of the particle, u_p the velocity of the particle, u the velocity of the fluid, F_{other} other interaction forces, $\dot{m}_p$ the particles mass flow rate and Δt the size of the time step.

The estimation of the pathline of each discrete-phase sand particle is performed by integrating the force balance on the particle. The particle inertia is equal to the forces acting on the particle. The particle inertia is equal to the forces acting on the particle. And in this case the drag force (F_D) is taken into account depending on the Reynolds number. F_D and Re can be written as:

$$F_D = \frac{18\mu C_D Re}{\rho_p d_p^2 24} \qquad (2)$$

$$Re = \frac{\rho d_p |\vec{u_p} - \vec{u}|}{\mu} \qquad (3)$$

The particle used for air+particle numerical tests has a diameter of 50 mm and a density of 2196 kg/m³.

Particle diameters, densities and volume fraction ratios used for the numerical tests dealt with regional environment system are also given in Table 2.

Table 2. Particle properties used in numerical tests

Material	Density (kg/m³)	Diameter (mm)
Particle (Sand)	2196.06	0.5/0.1/0.3

The reason for particle properties in Table 2 is that there is more than one particle between 1-500 µm in diameter in the air and it is more realistic to evaluate the environment with the particles of various concentrations, diameters and flow velocities in the air.

3 Results and discussion

In this study, it is aimed to determine the optimum aerodynamic performance characteristics of the NACA 0012 airfoil in different operating environments (air, air+particle). In order to determine these characteristics, numerical tests were carried out at different particle diameters, attack angles and Reynolds numbers.

In numerical tests, factors such as mesh structure and number, numerical algorithms, turbulence models used for turbulent flows, wall functions are effective on the results. Therefore, the numerical technique needs to be verified first.

In numerical tests, the results obtained with Re= 1.76×10^6, different angles of attack and different environments were compared with the results in the literature. The static pressure contours obtained from numerical tests at the boundary conditions specified in Figure 3 are given.
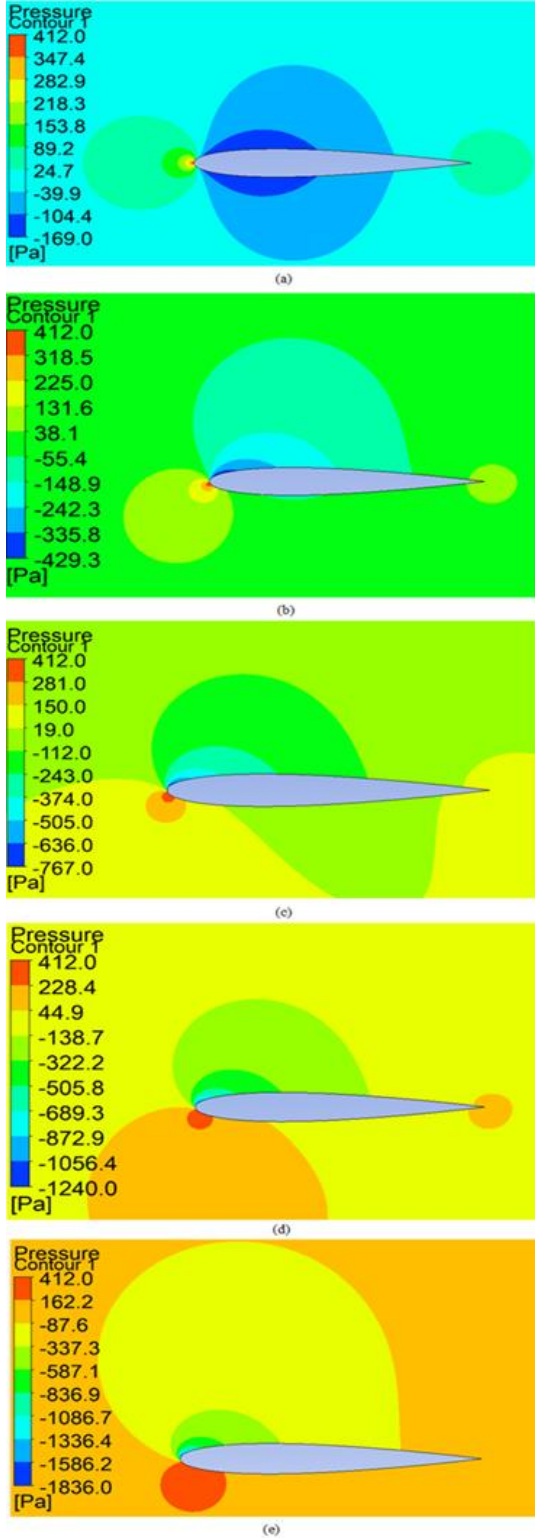

Figure 3. Contours of static pressure at (a) 0°, (b) 3°, (c) 5°, (d) 7° and (e) 9° angles of attack for air flow at Re=1.76×10^6

This value is in the range of 401-404 Pa in the Ref. Douvi et al. [20]. The maximum difference was obtained around 2.7%. In Figure 4, a comparison of the results obtained from the numerical tests for different angles of attack, Re= 1.76×10^6 and air-air+particle phases flow with the results in the literature [20-21] is given in order to evaluate the lift effects on the airfoil.
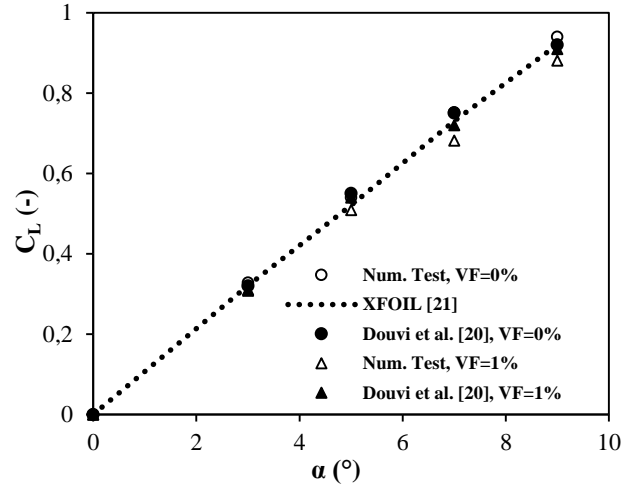

Figure 4. Comparison between literature [20-21] and numerical tests of the lift coefficient

As seen in Figure 4, the lift coefficient increases linearly with increasing angle of attack. This linear change continues until stall situations. This corresponds to angles of attack greater than 14° [20-21]. With the addition of 1% particles to air, there is a degradation in the lift coefficient.
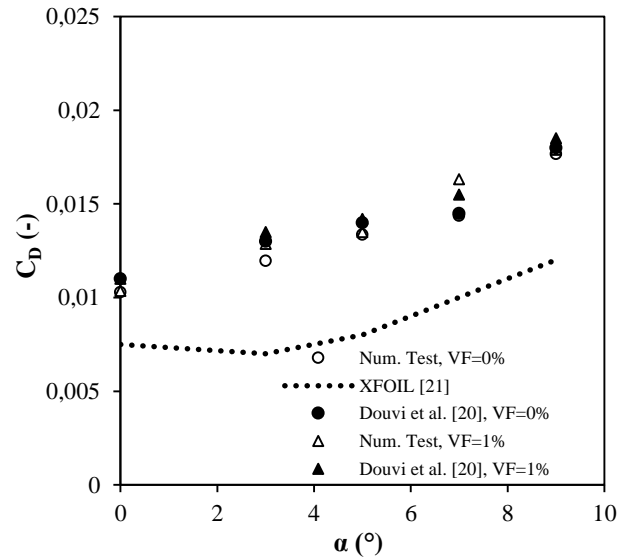

Figure 5. Comparison between literature [20-21] and Numerical tests of the drag coefficient

In Figure 5, a comparison of the results obtained from numerical tests for different angles of attack, Re= 1.76×10^6 and air-air+particle phases flow with the results in the literature [20-21] is given in order to evaluate the effects of

drag on the airfoil. As can be seen from this comparison, it is seen that the results obtained from the numerical tests are in harmony with the values in the literature [20-21]. The reason why the estimates obtained from numerical tests are higher than the theoretical results is due to the assumption that the flow is completely turbulent by using a turbulence model. With the addition of 1% particles to air, there is a slight increase in the drag coefficient due to the increase in surface friction forces.
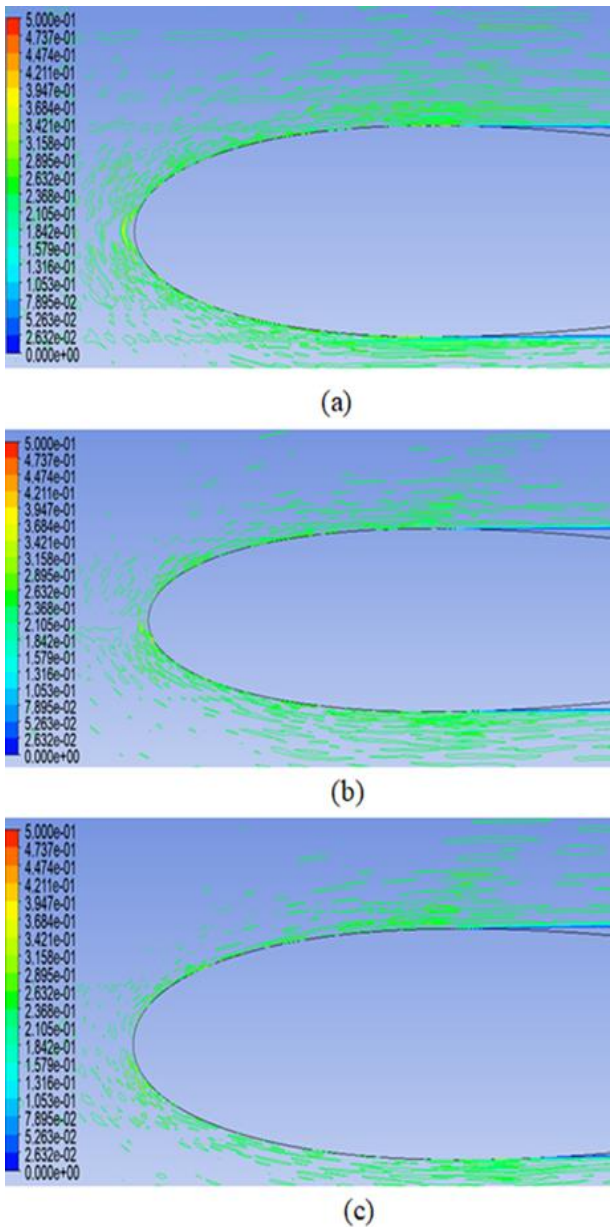

(a)

(b)

(c)

Figure 6. Comparison of contours of DPM concentration at (a) 0°, (b) 5° and (c) 9° angles of attack at Re=1.76x10^6 for 1% concentration of particle in the air

When the DPM contours are investigated, it is seen that the particle concentration is intensed on the front surface of the airfoil at 0° angle of attack, and this concentration shifts to the middle sections as the angle of attack increases (Figure 6).

The results obtained from the numerical tests for DPM concentration are in good agreement with the values in the literature [20].

After the numerical technique was verified with the results given in the literature, numerical tests were carried out in flow structures and environments with the particles of various concentrations, diameters and flow velocities in the air.
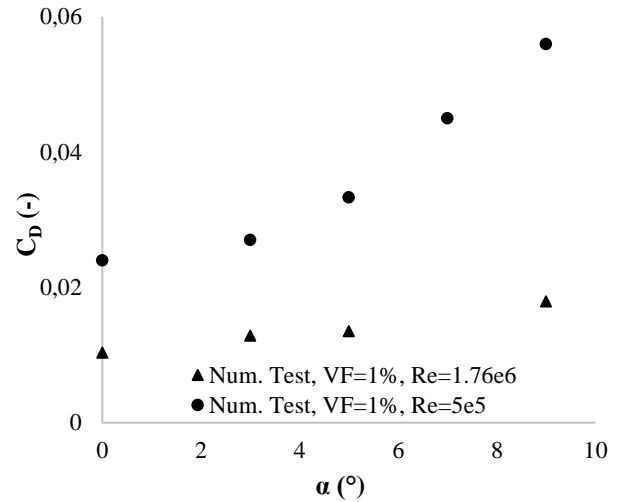

Figure 7. Comparison of drag coefficients for the air+particle (VF=1%) and the different attack angle around the airfoil for Re=1.76x10^6 and Re=5x10^5

In Figure 7, the comparison of drag coefficients for the air+particle (VF=1%) and the different attack angle around the airfoil for Re=1.76x10^6 and Re=5x10^5 is given. As can be clearly seen from this figure, the drag coefficient increases with decreasing Reynolds number. This is because viscous forces dominate over a large area of the airfoil.
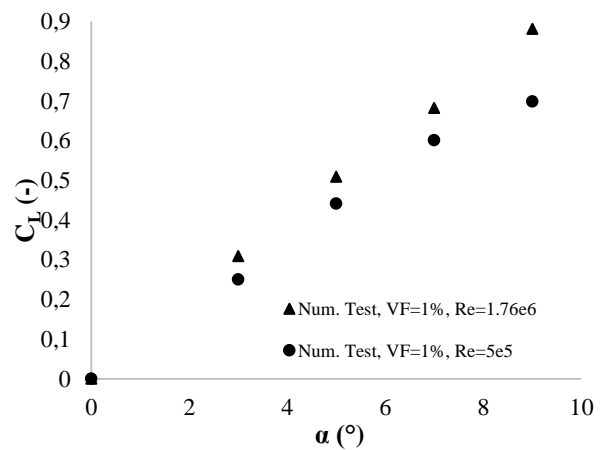

Figure 8. Comparison of lift coefficients for the air+particle (VF=1%) and the different attack angle around the airfoil for Re=1.76x10^6 and Re=5x10^5

Figure 8 gives the comparison of lift coefficients for the air+particle (VF=1%) and the different attack angle around the airfoil for Re=1.76x10^6 and Re=5x10^5. As can be clearly seen from this figure, the lift coefficient decreases with

decreasing Reynolds number. This is because viscous forces dominate over a large area of the airfoil.
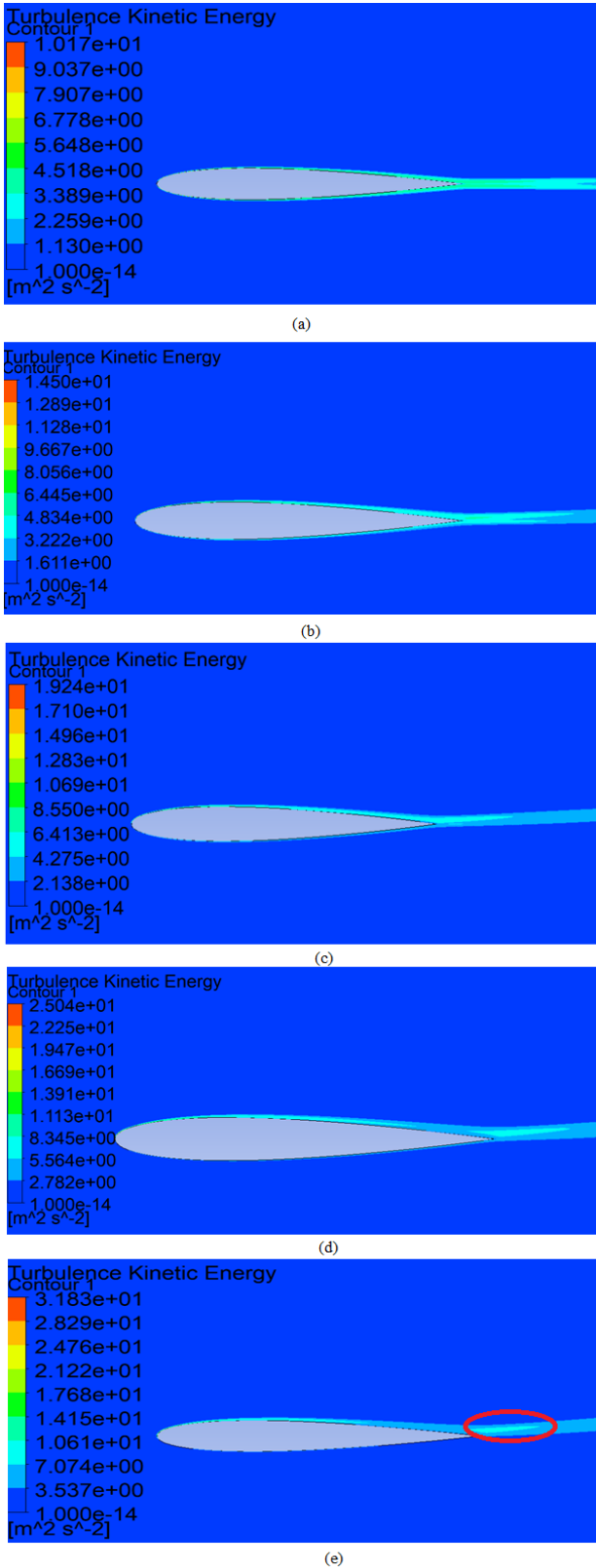

(a)

(b)

(c)

(d)

(e)

Figure 9. Contours of turbulence kinetic energy at (a) 0°, (b) 3°, (c) 5°, (d) 7° and (e) 9° angles of attack for air flow at Re=1.76x10^6

Turbulence kinetic energy is one of the most important parameters to determine the aerodynamic properties of the airfoil. Figure 9 gives the turbulent kinetic energies around the airfoil at different angles of attack for Re=1.76×10^6.

As can be seen in Figure 9 a, b and c, the turbulence kinetic energy value occurred in the tail region of the airfoil increases with the increase in the angle of attack and shifts towards the upper region of the airfoil at high attack angle. The region circled in red in Figure 9c shows that flow separation becomes evident at the 9° angle of attack. Because it is clearly seen that a weaker turbulent kinetic energy region occurs below this region.
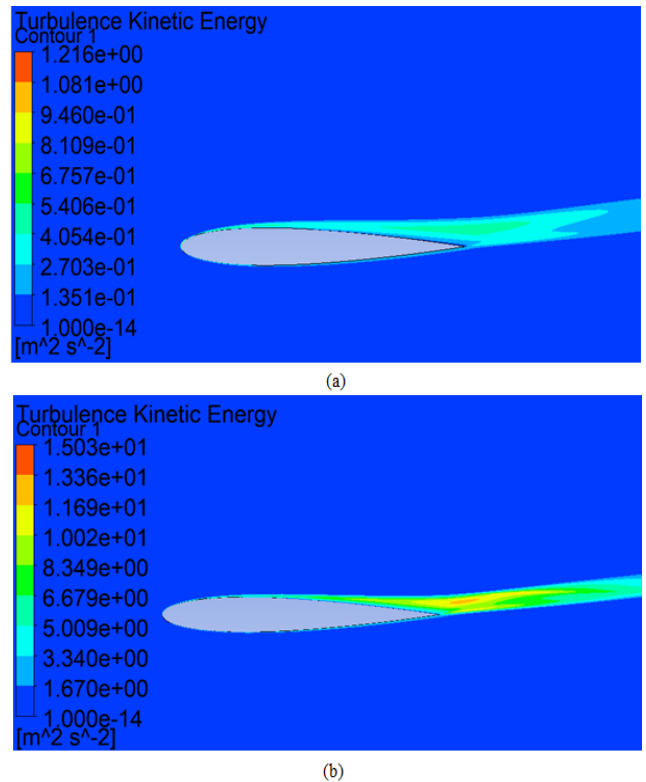

(a)

(b)

Figure 10. Contours of turbulence kinetic energy at (a) Re=5x10^5 and (b) Re=1.76x10^6 for 1% volume fraction ratio and 9° of attack angle

In Figure 10a in case of Re=5x10^5 and 9° angle of attack and in Figure 10b for the same conditions and Re=1.76x10^6, the turbulent kinetic energy contours for air+particle flow (VF=1%) around the airfoil are given. It is seen that the area and value of the separated region increase with the increase of the Reynolds number.

This is because the lift decreases and the drag increases with the increase of the viscous effects. Moreover, the area of the turbulent kinetic energy region, which is shifted from the tail region to the front of the airfoil at high angles of attack, becomes larger at low Reynolds numbers.

In Figure 11b, unlike Figure 11a, it is seen that the area and value of the separated region increase with the increase of the volume fraction ratio. This is because the lift decreases and the drag increases with the increase of the volume fraction ratio.
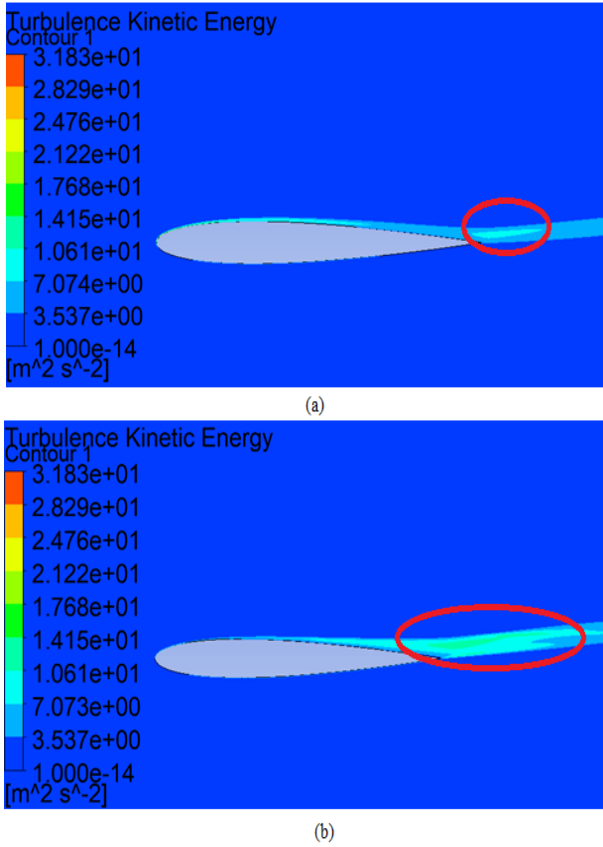
Figure 11. Contours of turbulence kinetic energy at (a) 0% and (b) 1% volume fraction ratios for flow at Re=1.76×10^6 and 9° of attack angle

In order to examine the effects of sand particle diameters specified in the literature on aerodynamic performance as well as the effects of particle concentration on aerodynamic performance, numerical tests were carried out at 1% volume fraction in 3 different particle diameters (Figure 12-13).
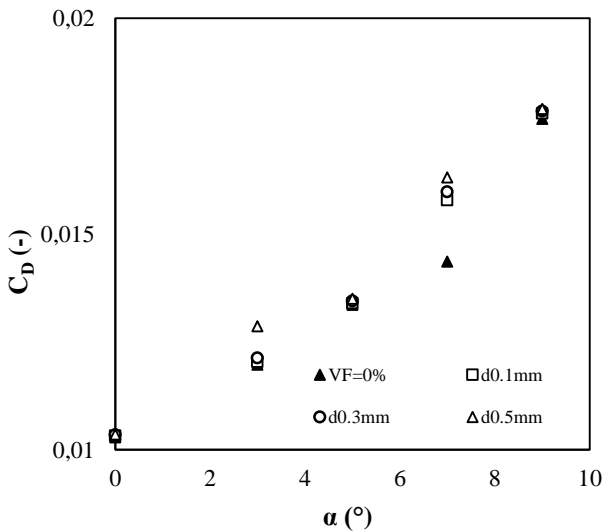

Figure 12. Comparison of Numerical tests of the drag coefficient obtained in different particle diameters at VF=1% and pure air (VF=0%)

Figure 12 is investigated, it is clearly seen that the presence of particle concentration in the pure air fluid has a direct and significant effect on the drag coefficient. In addition, the drag coefficient increases with the increase of particle diameter and angle of attack due to high skin friction.
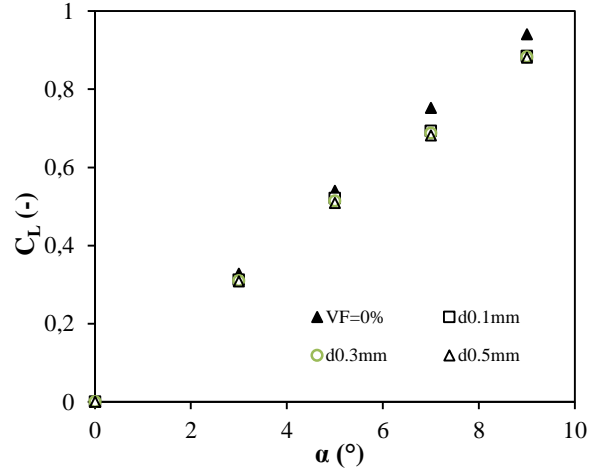

Figure 13. Comparison of Numerical tests of the lift coefficient obtained in different particle diameters at VF=1% and pure air (VF=0%)

The lift coefficient also decreases significantly with the presence of particles in pure air and with increasing particle diameter and angle of attack (Figure 13). This is reason due to the effect of gravitational forces.

When the numerical results obtained are evaluated, it can be stated that the drag and lift coefficients obtained in the numerical tests of the airfoils and in the experimental tests in the wind tunnel will differ from the values in the application area. Because, in the operation of airfoils in different regional environments, there are always particles of various concentrations and diameters in the air. In this case, the drag coefficient increases and the lift coefficient decreases.

4 Conclusion

This paper includes the investigation of turbulent kinetic energy structures formed during flow and the effects of the air containing the different diameters of particles and flow velocities in different regional areas on aerodynamic performance properties of NACA 0012.

The results obtained can be summarized as follows:

- Results obtained from the numerical tests for single and two phase fluid flow demonstrate good agreement with the value in the literature.
- Numerical test results indicate the turbulence kinetic energy value occurred in the tail region of the airfoil increases with the increase in the angle of attack and shifts towards the upper region of the airfoil at high attack angle. It is also seen that the area and value of the separated region increase with the increase of the Reynolds number. Moreover, the upper region of the airfoil at high attack angle becomes larger at low Reynolds numbers due to viscous effects.

- This paper recommended that the drag and lift coefficients obtained in the numerical tests of the airfoils and in the experimental tests in the wind tunnel will differ from the values in the application area. The reason for this is that there are always particles of varying concentrations and diameters in the air in different regional environments.
- It can be stated that the presence of particles in the air, even at very low particle concentrations, has a negative effect on aerodynamic performance.

Conflict of interest

The author declares that there is no conflict of interest.

Similarity rate (iThenticate): %17

References

[1] R.L. Fearn, Airfoil aerodynamics using panel methods, The Mathematica Journal, 10(4), 1-17, 2008. https://dx.doi.org/10.3888/tmj.10.4-6.

[2] C. E. Douvi, I. A. Tsavalos and P. D. Margaris, Evaluation of the turbulence models for the simulation of the flow over a National Advisory Committee for Aeronautics (NACA) 0012 airfoil, Journal of Mechanical Engineering Research, 4(3), 100-111, 2012. https://doi.org/10.5897/JMER11.074

[3] M. Adel, A comparative study for different shapes of airfoils, International Journal of Mechanical Engineering, 4, 27-39, 2019.

[4] A. Bodavula, U. Guven and R. Yadav, Numerical analysis of protrusion effect over an airfoil at Reynolds Number 10^{-5}, International Journal of Recent Technology and Engineering, 8(2), 2583-2588, 2019.

[5] V. Iliev, M. Lazareviki and V. Aleksoski, Numerical and experimental investigation of airfoil performance in a wind tunnel, American Journal of Engineering Research, 9(4), 119-124, 2020.

[6] J. C. M. Lin and L. L. Pauley, Low-Reynolds-number separation on an airfoil, AIAA Journal, 34(8), 1570-1577, 1996. https://doi.org/10.2514/3.13273

[7] A. Choudhry, M. Arjomandi and R. Kelso, A study of long separation bubble on thick airfoils and its consequent effects, International Journal of Heat and Fluid Flow, 52, 84-96, 2015. https://doi.org/10.1016/j.ijheatfluidflow.2014.12.001

[8] P. Jimenez, P. Lichota, D. Agudelo and K. Rogowski, Experimental validation of total energy control system for UAVs, Energies, 13(14), 1-18, 2020. https://doi.org/10.3390/en13010014

[9] K. Rogowski, G. Królak and G. Bangga, Numerical study on the aerodynamic characteristics of the NACA 0018 airfoil at low Reynolds Number for Darrieus wind turbines using the transition SST model, Processes, 9(3), 477, 2021. https://doi.org/10.3390/pr9030477

[10] M. Umapathi and N. Soni, Comparative analysis of airfoil NACA 2313 and NACA 7322 using computational fluid dynamics method, International Journal of Scientific Progress and Research, 12(04), 193-198,2015.

[11] N. Singh, Analysis of aerodynamic characteristics of various airfoils at sonic speed, International Journal of Engineering Research & Technology, 5(9), 405-411, 2016.

[12] R. I. Rubel, M. K. Uddin, M. Z. Islam and M. Rokunuzzaman, Comparison of aerodynamics aharacteristics of NACA 0015 & NACA 4415 aerofoil blade, International Journal of Research-Granthaalayah, 5(11), 187-197, 2017. https://doi.org/10.20944/preprints201610.0095.v1

[13] R. I. Pranto and M. I. Inam, Numerical analysis of the aerodynamic characteristics of NACA-4312 airfoil, Journal of Engineering Advancements, 01(02), 29-36, 2020.

[14] V. Dhiyyadharshini, R. Krishna and V. Kamaleshwari, Investigation of aerodynamic efficiency on NACA 2412 airfoil, International Journal of Engineering Research & Technology, 10(9), 725-728, 2021.

[15] A. Shabur, A. Hasan and M. Ali, Comparison of aerodynamic behaviour between NACA 0018 and NACA 0012 airfoils at low Reynolds Number through CFD analysis, Advancement in Mechanical Engineering and Technology, 3(2), 1-8,2020. https://doi.org/10.5281/zenodo.4003677

[16] H. Fatahian, H. Salarian, M. E. Nimvari and J. Khaleghinia, Numerical simulation of the efect of rain on aerodynamic performance and aeroacoustic mechanism of an airfoil via a two-phase fow approach, Applied Sciences, 2(5), 867, 2020. https://doi.org/10.1007/s42452-020-2685-4

[17] P. Haines and J. Luers, Aerodynamic penalties of heavy rain on landing airplanes, Journal of Aircraft, 20(2), 111-119, 1983. https://doi.org/10.2514/3.44839

[18] Y. Cao, Z. Wu and Z. Xu, Effects of rainfall on aircraft aerodynamics, Progress in Aerospace Sciences, 71, 85-217, 2014. https://doi.org/10.1016/j.paerosci.2014.07.003

[19] Z. Wu and Y. Cao, Numerical simulation of flow over an airfoil in heavy rain via a two-way coupled Eulerian–Lagrangian approach, International Journal of Multiphase Flow, 69, 81-92, 2015. https://doi.org/10.1016/j.ijmultiphaseflow.2014.11.006

[20] D. C. Douvi, E. C. Douvi and D. P. Margaris, Computational study of NACA 0012 airfoil in air-sand particle two-phase flow at Reynolds Number of Re=1.76×10^6, International Journal of New Technology and Research, 5(4), 101-108, 2019. https://doi.org/10.31871/IJNTR.5.4.18

[21] M. Drela, XFOIL: An analysis and design system for low Reynolds Number airfoils, Springer-Verlag, 54, 1-12, 1989. https://doi.org/10.1007/978-3-642-84010-4_1.